Phase Separation of YAP Reprograms Cells for Long-term YAP Target Gene Expression

Danfeng Cai[1], Shahar Sukenik[2, †], Daniel Feliciano[3, ††], Martin Gruebele[2], Jennifer Lippincott-Schwartz[1, 3, *]

[1]Eunice Kennedy Shriver National Institute for Child Health and Human Development, National Institute of Health, Bethesda, Maryland 20892
[2]Department of Chemistry, University of Illinois at Urbana–Champaign, Urbana, Illinois 61801
[3]Janelia Research Campus, Howard Hughes Medical Institute, Ashburn, Virginia 20147

*Correspondence to: lippincottschwartzj@janelia.hhmi.org

[†]Current address: Department of Chemistry and Chemical Biology, University of California at Merced, 5200 N Lake Dr, Merced, CA 95340
[††]Current address: Thoracic and Malignancies Branch, National Cancer Institute, National Institute of Health, Bethesda, Maryland 20892

Abstract

Yes-associated Protein (YAP) regulates cell proliferation and survival, and is over-expressed in most malignant tumors. As a transcriptional co-activator, its nuclear localization is the key determinant of its function. Recent work has revealed that hyperosmotic stress leads to YAP nuclear translocation and target gene expression, but how this overrides canonical YAP regulation by the Hippo pathway is unclear. Here we showed that YAP has an intrinsic ability to form liquid-like condensates when macromolecular crowding inside a cell increases, and this caused YAP to translocate to the nucleus, initiating downstream YAP signaling. Within seconds of inducing macromolecular crowding by hyperosmotic stress, YAP partitioned into cytoplasmic and nuclear droplets. Cytoplasmic YAP droplets concentrated YAP into an environment where it could be phosphorylated by NLK for nuclear translocation, whereas YAP nuclear droplets (enriched in TEAD1 and TAZ) functioned to re-organize gene enhancer elements, readying transcription of proliferation genes once the cell had either adapted to or been relieved of hyperosmotic stress. Thus, principles of liquid phase partitioning are used for reprogramming cells into a YAP-dependent, proliferative state in response to macromolecular crowding.

Macromolecular crowding is a key feature of all eukaryotic cells, helping to drive polypeptide chains to fold into functional proteins, and impacting the diffusion and reaction kinetics of molecules. When molecular crowding inside a cell reaches a threshold, it can induce a process called liquid-liquid phase separation (LLPS)[1, 2], in which labile, multivalent interactions among proteins and/or RNAs leads to their demixing from the surrounding milieu into liquid-like or gel-like condensates[3-5]. While the effects of macromolecular crowding on diffusion/reaction kinetics and protein phase separation have been studied *in vitro*, very little is known about how molecular crowding regulates general cell physiological processes, where changes in macromolecular crowding are known to occur. For example, changes in macromolecular crowding occur during starvation[6], cell division[7], and when cells experience differences in substrate stiffness[8]. Changes in macromolecular crowding also occur in cells of kidney[9], gut[10, 11] and blood vessels[12], when they undergo changes in osmotic pressure. What specific signaling pathways are triggered by these changes in macromolecular crowding to help the cell adapt to and survive in its transformed environment are unknown.

Recently, hyperosmotic stress, which increases macromolecular crowding[13, 14], has been shown to increase the nuclear localization of YAP, a key controller of organ size in animals. As a transcriptional co-activator, YAP is normally controlled by Hippo pathway. When the Hippo pathway is active, YAP binds to 14-3-3 proteins and is retained in the cytoplasm. When the Hippo pathway is inactive, YAP is freed from binding to 14-3-3 proteins and redistributes into the nucleus, where it triggers transcription of proliferation-specific genes with the TEA domain family member (TEAD) transcription factors[15, 18, 19].

However, hyperosmotic stress was found to cause YAP nuclear localization and target gene expression, overriding canonical Hippo pathway regulation[17]. Given YAP's significance in controlling multiple aspects of cell behavior, including proliferation, cell stemness and malignancy[15, 20, 21], we sought to investigate how increase in macromolecular crowding mediated by hyperosmotic stress leads to YAP activation.

To study the mechanism by which macromolecular crowding regulates YAP activity, we treated U2-OS cells transiently expressing EGFP-YAP with 10% w/v PEG-300 (PEG), an osmotic stressor. Cytoplasmic and nuclear volume decreased by 22 ± 7 % and 32 ± 9 % respectively (Fig. 1a, b), resulting in the cells having a more crowded intracellular environment (Fig. 1c) and higher dry mass density[22] (Extended Data Fig. 1a). In response to this treatment, EGFP-YAP signal redistributed into the nucleus, peaking at 10 min before attaining a steady state nuclear concentration that, while lower than at 10 min, was higher than that seen before PEG treatment (Fig. 1d). Similar results were seen for endogenous YAP (Extended Data Fig. 1b). Washout of PEG resulted in EGFP-YAP's signal quickly returning to its predominantly cytoplasmic, pre-treatment localization (Fig. 1d), indicating that the process is highly reversible. Within 3 h of PEG treatment, transcription of YAP target genes was increased by 2-fold (Fig. 1e), indicating that YAP's nuclear redistribution led to downstream target gene expression, as previously reported[17].

Visualizing EGFP-YAP dynamics under hyperosmotic stress more closely, we found that YAP changed from being diffusely distributed in the cytoplasm to being localized in

discrete cytoplasmic and nuclear puncta within 15-30 s of adding PEG (Fig. 2a, upper panel and Movie S1). In zoomed-in images, these appeared spherical (Fig. 2b). This contrasted with the behavior of EGFP (Fig. 2a, lower panel) or EGFP-RhoA (Extended Data Fig. 2a) expressed in cells, which showed no change in subcellular distribution upon hyperosmotic stress. The EGFP-YAP puncta persisted for 10-15 min before slowly dissipating. Washing in isotonic medium when the puncta were still present caused the puncta to disappear in 30 seconds (Fig. 2a, upper panel, Movie S1). The foci were not artifacts of EGFP-YAP overexpression, since endogenous YAP-positive foci labeled by YAP antibody staining could be seen after PEG treatment in cells not expressing EGFP-YAP (Extended Data Fig. 2b). The formation of YAP foci was cell type-independent (Extended Data Fig. 2c), YAP isoform-independent (Extended Data Fig. 2d), and not limited to specific osmotic agent used (Extended Data Fig. 2e).

Protein and RNA can partition into discrete fluid condensates in the process called liquid-liquid phase separation when they reach a local concentration threshold mediated by weak multivalent interactions[2, 5, 23]. These so-called 'liquid droplets' have spherical shapes, can coalesce into larger structures, and can exchange their contents with the rest of the cytosol or within the structure[3]. We found that YAP foci exhibited similar properties. They showed high sphericity in high resolution images (Extended Data Fig. 2f), could fuse with each other to form larger spheres in both the nucleus and the cytoplasm (Fig. 2c, Movie S2-S4), and exhibited rapid fluorescence recovery upon photobleaching either the entire foci ($t_{1/2} = 0.9 \pm 0.4$ sec, Fig. 2d, e) or part of one (Fig.

2f). Therefore, YAP foci formed under hyperosmotic stress are genuine phase-separated liquid droplets.

To determine whether YAP's ability to condense into liquid droplets is an intrinsic property or requires other co-factors, we expressed and purified EGFP-YAP from *E. coli* and examined EGFP-YAP's behavior under different conditions. Non-ionic crowders larger than 300Da produced a turbid EGFP-YAP solution and this was dependent on both the concentration of EGFP-YAP and concentration and size of PEG (Fig. 3a). Confocal imaging of the turbid EGFP-YAP solution revealed micron-sized spheres that displayed liquid-like characteristics (Fig. 3b), including droplet coalescence (Fig. 3c), wetting the coverslip (Movie S5) and concentration-dependent recovery after photobleaching (Fig. 3d), as reported for proteins capable of phase partitioning[24]. The purified EGFP-YAP droplets retained their fluidity over 30 min and did not undergo irreversible aggregation (Extended Data Fig. 3b). EGFP-YAP droplets disappeared when the solution was re-suspended in 20mM Tris buffer, indicating their formation was reversible (Fig. 3b, washed). Other conditions known to affect protein phase separation (i.e., salts, inert proteins, and nucleic acids)[24, 25] did not trigger YAP droplet formation (Extended Data Fig. 3a). Indeed, varying salt concentration failed to change the turbidity of EGFP-YAP solution, suggesting that strong electrostatic interactions don't play an important role in YAP phase separation (Extended Data Fig. 3a). UV circular dichroism (CD) analysis revealed the presence of possible α-helical structure in YAP condensates (Fig. 3e), indicating that weak multivalent interactions among coiled-coil structures might help drive YAP's co-acervation into droplets under crowded conditions. These data

indicate that under macromolecular crowding YAP has an intrinsic ability to partition into liquid condensates through a mechanism independent of salts or nucleic acids.

Phase-separated condensates provide cells with an additional way to organize their internal space, functioning as hubs to facilitate protein-protein interactions or to sequester proteins away from their normal partners[3]. With this in mind, we examined what other proteins co-segregate with YAP in YAP-enriched droplets seen under hyperosmotic stress. Focusing first on cytoplasmic YAP droplets, we concluded they were not stress granules because they neither contained the stress granule component G3BP (Extended Data Fig. 4a) nor co-segregated with G3BP-containing stress granules under arsenite treatment (Extended Data Fig. 4b). YAP droplets also were not processing bodies (P-bodies) involved in RNA processing as they lacked critical P-body components, including GW182 and Ago2 (Extended Data Fig. 4c, d). However, the P-body component Dcp1a did co-segregate with YAP droplets (Fig. 4a, d), suggesting some unknown link to RNA processing. Intriguingly, YAP droplets contained proteins involved in YAP-specific post-translational modifications, including Nemo-like kinase (NLK) (Fig. 4b, d) and Hippo pathway kinase large tumor suppressor 1 (LATS1) (Fig. 4c, e). NLK phosphorylates YAP on Serine 128, releasing YAP from 14-3-3 protein association thereby triggering its nuclear re-localization[17, 26]. Co-segregation of NLK and YAP in droplets thus could facilitate this reaction, leading to YAP nuclear redistribution. Co-segregation of LATS1 with YAP in droplets seemed at odds with NLK's role because LATS1 phosphorylates YAP at Serine 127, an event that leads to tighter association of YAP with 14-3-3 proteins[18, 27]. However, MST2, one of the kinases that activates LATS1

to enable its phosphorylation of YAP, did not localize to YAP droplets (Extended Data Fig. 4e). YAP droplet association of LATS1 thus might sequester LATS1 away from MST2, leading to decreased LATS1 activity. These findings show that YAP condensates are neither stress granules nor P-bodies, but are a novel type of cytoplasmic droplet that sequesters kinases that target YAP for possible nuclear translocation.

We next investigated what molecules co-segregate with YAP condensates in the nucleus, hoping to gain clues as to the roles of YAP in this environment. YAP nuclear condensates did not co-localize with known nuclear body markers such as SC35 (nuclear speckle, Extended Data Fig. 4f), PML (promyelocytic leukemia bodies, Extended Data Fig. 4g), or Coilin (Cajal bodies, Extended Data Fig. 4h), suggesting they perform functions different from these well-known nuclear bodies. Notably, YAP condensates were enriched in the transcription factor TEAD1 (Fig. 4f, j) and another coactivator of the YAP/TAZ signaling pathway, TAZ (Extended Data Fig. 4i). They also were enriched in β-catenin, the transcription coactivator of the Wnt signaling pathway that is often co-regulated with YAP[28-30] (Fig. 4g, j). These properties of nuclear YAP droplets were similar to phase-separated structures in the nucleus called super enhancers (SEs)[31, 32], which contain gene enhancer elements in clusters that are close with each other and the promoters of genes they regulate[33-35].

To gain more insight into the function of nuclear YAP droplets, we probed them with antibodies to RNA Pol II, discovering that RNA Pol II separated away from YAP nuclear

droplets upon hyperosmotic shock (Fig. 4h, j). YAP nuclear droplets also did not overlap with nascent connective tissue growth factor (Ctgf) RNA as shown by RNA-FISH (Fig. 4i). This suggests that YAP nuclear droplets, while potentially driving clustering of gene enhancer elements to form SEs, do not recruit RNA Pol II. This could be important for preventing transcriptional activity at these super enhancer sites in the initial phase of hyperosmotic shock. Our RT-PCR results showing an initial decrease at 20 min in YAP signaling upon hyperosmotic shock (see Fig. 1e) is consistent with this possibility. We thus hypothesized that only later, when YAP droplets have disappeared as visible structures, would newly formed, YAP-induced SEs impact cell reprograming by recruiting RNA Pol II, leading to rapid transcription of cell proliferation genes. Supporting this possibility, we observed that treating cells with PEG for just 10 min was enough to confer cells with a proliferation advantage 2 hours later compared with cells in normal medium, as shown by EdU labeling (Fig. 4k). A recent paper reported that hyperosmotic shock depletes RNA Pol II from promoter regions of genes, and after relieving cells of hyperosmotic stress, cells accumulate more Pol II at promoter regions than before treatments[36]. Our results confirmed this finding, and further suggested that it is YAP nuclear droplets that re-organize gene enhancer elements to facilitate rapid transcription of cell proliferation genes once cells have either adapted to or been relieved of hyperosmotic stress.

We next sought to identify and remove regions in YAP responsible for its phase separation under hyperosmotic stress to test whether YAP droplet formation is necessary for the above effects on transcription and DNA synthesis. The YAP protein

mainly consists of disordered sequences except for the central WW domain and C-terminal PDZ binding motif (Fig. 5a). To identify regions responsible for YAP phase separation, we first deleted the C-terminal transcriptional activation domain (TAD) of YAP and made an EGFP-YAPΔTAD fusion protein (Fig. 5b). We found that EGFP-YAPΔTAD was unable to phase separate under hyperosmotic shock (Fig. 5c, d), indicating that the TAD sequence is indispensable for YAP phase separation. We further found that phase separation-deficient EGFP-YAPΔTAD disrupts endogenous YAP droplet formation (Extended Data Fig. 5), and has impaired nuclear localization compared with wildtype (WT) EGFP-YAP at 15 min after PEG treatment (Fig. 5e). To test whether YAP phase separation seen immediately after PEG addition is necessary for the long-term promotion of YAP transcriptional activity, we expressed EGFP-YAP-ΔTAD in U2-OS cells and studied the localization of endogenous TEAD1 transcription factor. In the absence of YAP liquid droplets, TEAD1 did not enrich in any nuclear foci (Fig. 5f). Correspondingly, the transcriptional activity of YAP under hyperosmotic stress was much decreased in cells expressing ΔTAD compared to those expressing WT-YAP as assessed by Ctgf mRNA expression 3 hrs after PEG treatment (Fig. 5g), indicating that formation of liquid droplets enhances YAP target gene transcription in the long run. These results indicated that the C-terminal TAD domain was necessary for YAP condensate formation, and that the formation of YAP condensates was required for downstream YAP signaling.

The N-terminal 51 amino acid region of YAP is a low complexity proline-rich domain (comprised of 35% proline) (Fig. 5b), which might enhance the solubility of YAP

condensates (i.e., preventing their gelation) by acting as a hydrophilic agent[37, 38]. Consistent with this possibility, deletion of this region did not inhibit formation of YAP liquid droplets. Rather, the EGFP-YAPΔP condensates persisted longer in the cell, being visible 15 min after PEG treatment when the EGFP-YAP full length condensates had already disappeared (Fig. 5c, d). These results indicate that only the C-terminal TAD was responsible for YAP condensate formation, with other disordered sequences in the protein (i.e., proline-rich domain) acting to maintain fluidity of the condensates.

In conclusion, we describe a mechanism for how hyperosmotic stress causes YAP to translocate to the nucleus and initiate downstream YAP signaling that is based on YAP's intrinsic ability to phase partition into liquid droplets under macromolecular crowding. In this mechanism, YAP's low complexity TAD domain causes YAP to partition into cytoplasmic and nuclear droplets within seconds of increased macromolecular crowding. Whereas cytoplasmic YAP droplets concentrate YAP into an environment where it becomes modified for nuclear translocation, YAP nuclear droplets (enriched in TEAD1, TAZ and β-catenin) function to re-organize gene enhancer elements, readying transcription of proliferation genes once the cell has either adapted to or been relieved of hyperosmotic stress. Transient nuclear YAP droplet formation under increased macromolecular crowding thus represents a novel way that cells reprogram their long-term gene expression patterns. Its operation may be relevant for understanding cell state changes under various physiological conditions where macromolecular crowding increases.

References and Notes:

1. Delarue, M. *et al.* mTORC1 Controls Phase Separation and the Biophysical Properties of the Cytoplasm by Tuning Crowding. *Cell* **174**, 338-+ (2018).
2. Woodruff, J.B. *et al.* The Centrosome Is a Selective Condensate that Nucleates Microtubules by Concentrating Tubulin. *Cell* **169**, 1066-+ (2017).
3. Shin, Y. & Brangwynne, C.P. Liquid phase condensation in cell physiology and disease. *Science* **357** (2017).
4. Banani, S.F., Lee, H.O., Hyman, A.A. & Rosen, M.K. Biomolecular condensates: organizers of cellular biochemistry. *Nat Rev Mol Cell Biol* **18**, 285-298 (2017).
5. Jain, A. & Vale, R.D. RNA phase transitions in repeat expansion disorders. *Nature* **546**, 243-+ (2017).
6. Joyner, R.P. *et al.* A glucose-starvation response regulates the diffusion of macromolecules. *Elife* **5** (2016).
7. Son, S. *et al.* Resonant microchannel volume and mass measurements show that suspended cells swell during mitosis. *Journal of Cell Biology* **211**, 757-763 (2015).
8. Guo, M. *et al.* Cell volume change through water efflux impacts cell stiffness and stem cell fate. *P Natl Acad Sci USA* **114**, E8618-E8627 (2017).
9. Sheikh-Hamad, D. & Gustin, M.C. MAP kinases and the adaptive response to hypertonicity: functional preservation from yeast to mammals. *Am J Physiol Renal Physiol* **287**, F1102-1110 (2004).
10. Shiau, Y.F., Feldman, G.M., Resnick, M.A. & Coff, P.M. Stool electrolyte and osmolality measurements in the evaluation of diarrheal disorders. *Ann Intern Med* **102**, 773-775 (1985).
11. Klaschik, E., Nauck, F. & Ostgathe, C. Constipation--modern laxative therapy. *Support Care Cancer* **11**, 679-685 (2003).
12. Jacob, M., Chappell, D. & Becker, B.F. Regulation of blood flow and volume exchange across the microcirculation. *Crit Care* **20**, 319 (2016).
13. Miermont, A. *et al.* Severe osmotic compression triggers a slowdown of intracellular signaling, which can be explained by molecular crowding. *P Natl Acad Sci USA* **110**, 5725-5730 (2013).
14. Finan, J.D. & Guilak, F. The effects of osmotic stress on the structure and function of the cell nucleus. *J Cell Biochem* **109**, 460-467 (2010).
15. Pan, D. The hippo signaling pathway in development and cancer. *Dev Cell* **19**, 491-505 (2010).
16. Totaro, A., Panciera, T. & Piccolo, S. YAP/TAZ upstream signals and downstream responses. *Nat Cell Biol* **20**, 888-899 (2018).
17. Hong, A.W. *et al.* Osmotic stress-induced phosphorylation by NLK at Ser128 activates YAP. *Embo Reports* **18**, 72-86 (2017).
18. Dong, J.X. *et al.* Elucidation of a universal size-control mechanism in Drosophila and mammals. *Cell* **130**, 1120-1133 (2007).
19. Meng, Z., Moroishi, T. & Guan, K.L. Mechanisms of Hippo pathway regulation. *Genes Dev* **30**, 1-17 (2016).
20. Zanconato, F., Cordenonsi, M. & Piccolo, S. YAP/TAZ at the Roots of Cancer. *Cancer Cell* **29**, 783-803 (2016).

21. Lian, I. *et al.* The role of YAP transcription coactivator in regulating stem cell self-renewal and differentiation. *Gene Dev* **24**, 1106-1118 (2010).
22. Wang, Z. *et al.* Spatial light interference microscopy (SLIM). *Opt Express* **19**, 1016-1026 (2011).
23. Shin, Y. *et al.* Spatiotemporal Control of Intracellular Phase Transitions Using Light-Activated optoDroplets. *Cell* **168**, 159-+ (2017).
24. Lin, Y., Protter, D.S.W., Rosen, M.K. & Parker, R. Formation and Maturation of Phase-Separated Liquid Droplets by RNA-Binding Proteins. *Mol Cell* **60**, 208-219 (2015).
25. Smith, J. *et al.* Spatial patterning of P granules by RNA-induced phase separation of the intrinsically-disordered protein MEG-3. *Elife* **5** (2016).
26. Moon, S. *et al.* Phosphorylation by NLK inhibits YAP-14-3-3-interactions and induces its nuclear localization. *EMBO Rep* **18**, 61-71 (2017).
27. Hao, Y.W., Chun, A., Cheung, K., Rashidi, B. & Yang, X.L. Tumor suppressor LATS1 is a negative regulator of oncogene YAP. *J Biol Chem* **283**, 5496-5509 (2008).
28. Benham-Pyle, B.W., Pruitt, B.L. & Nelson, W.J. Cell adhesion. Mechanical strain induces E-cadherin-dependent Yap1 and beta-catenin activation to drive cell cycle entry. *Science* **348**, 1024-1027 (2015).
29. Azzolin, L. *et al.* YAP/TAZ incorporation in the beta-catenin destruction complex orchestrates the Wnt response. *Cell* **158**, 157-170 (2014).
30. Konsavage, W.M., Jr. & Yochum, G.S. Intersection of Hippo/YAP and Wnt/beta-catenin signaling pathways. *Acta Biochim Biophys Sin (Shanghai)* **45**, 71-79 (2013).
31. Cho, W.K. *et al.* Mediator and RNA polymerase II clusters associate in transcription-dependent condensates. *Science* (2018).
32. Sabari, B.R. *et al.* Coactivator condensation at super-enhancers links phase separation and gene control. *Science* (2018).
33. Chong, S.S. *et al.* Imaging dynamic and selective low-complexity domain interactions that control gene transcription. *Science* **361**, 378-+ (2018).
34. Hnisz, D., Shrinivas, K., Young, R.A., Chakraborty, A.K. & Sharp, P.A. A Phase Separation Model for Transcriptional Control. *Cell* **169**, 13-23 (2017).
35. Hnisz, D. *et al.* Super-Enhancers in the Control of Cell Identity and Disease. *Cell* **155**, 934-947 (2013).
36. Erickson, B., Sheridan, R.M., Cortazar, M. & Bentley, D.L. Dynamic turnover of paused Pol II complexes at human promoters. *Genes Dev* **32**, 1215-1225 (2018).
37. Crick, S.L., Ruff, K.M., Garai, K., Frieden, C. & Pappu, R.V. Unmasking the roles of N- and C-terminal flanking sequences from exon 1 of huntingtin as modulators of polyglutamine aggregation. *P Natl Acad Sci USA* **110**, 20075-20080 (2013).
38. Bergeron-Sandoval, L.P., Safaee, N. & Michnick, S.W. Mechanisms and Consequences of Macromolecular Phase Separation. *Cell* **165**, 1067-1079 (2016).

Acknowledgements:
We are grateful to the thoughtful discussions with Duojia Pan (UTSW), Ming Guo (MIT), and members of the Lippincott-Schwartz laboratory.

Funding:
This work was supported by the Intramural Research Program of the National Institutes of Health (J.L.-S., D.C.), the Howard Hughes Medical Institute (J.L.-S.), and Damon Runyon Cancer Research Fellowship (D.C. DRG2233-15), as well as NSF MCB 1803786 (S.S. and M.G.).

Authors Contributions:
D.C. and J.L.-S. conceived the project and designed the study. D.C. performed all the experiments in cell. S.S. performed all the experiments *in vitro*. D. F. constructed mutant constructs for experiments. J.L.-S. and M.G. supervised research, interpreted data, and participated in project planning. D.C. and J.L.-S. wrote the manuscript with inputs from all the authors.

Competing Interests:
The authors have no competing interests.

Data and materials availability:
All data is available in the main text or the supplementary materials.

Figure Legends:

Fig. 1. Cells change volume and form YAP-positive condensates during hyperosmotic stress. (a) Side-view of a cell before, undergoing, and after hyperosmotic stress, 3-D rendered by Imaris. Color bar: volume (μm^3). (b) Quantification of normalized U2-OS nuclear (cyan), cytoplasmic (pink) and total (blue) volume. Unpaired t test. Comparing to volume before treatment. EGFP-YAP cellular localization in a U2-OS cell at indicated time. (c) Ratiometric images and quantification of crowding sensor FRET expressed in U2-OS cells. Rainbow-RGB showing changes in FRET indices. Color bar: FRET index (a.u.). (d) Localization of EGFP-YAP in U2-OS cells and quantification of normalized nuclear to cytoplasmic EGFP-YAP ratio. Unpaired t test. Comparing to ratio pre-treatment. (e) Relative Ctgf and Cyr61 mRNA levels in control and PEG-treated HEK 293T cells expressing EGFP-YAP. Unpaired t test. Error bars are SEM. *p<0.05, **p<0.01, ***p<0.001, ****p<0.0001. Scale bars are 5μm.

Fig. 2. YAP condensates have liquid-like properties in cell. (a) EGFP-YAP forms cytoplasmic and nuclear foci 15 sec after PEG treatment and disappears after wash, while EGFP alone doesn't. Scale bar: 5μm (b) Nuclear and cytoplasmic YAP condensates. Scale bar: 2μm. (c) Fusion of nuclear and cytoplasmic EGFP-YAP droplets. (d) FRAP recovery image of nuclear or cytoplasmic EGFP-YAP droplet. Dotted circle: Spot of photobleaching. Scale bars in c and d are 1μm. (e-f) Nuclear FRAP recovery curve when whole droplet (e) or part of the droplet (f) is bleached. Error bars in e, f are SD.

Fig. 3. Purified YAP condensates have liquid-like properties in vitro. (a) Purified EGFP-YAP shows concentration-dependent increase in turbidity at increasing wt% of PEG1000 and PEG6000. Color bar: turbidity measured at 600nm (a.u.). (b) EGFP-YAP pre-treatment (left) and after the addition of 25% PEG (middle). Upon centrifugation and resuspension in buffer, the droplets disappear (right). Scale bar, 10μm. (c) Droplet coalescence shown in fluorescence (top) and brightfield (bottom) illumination. Scale bar, 2μm. (d) Spot-bleach FRAP experiment show that the recovery in the bleached spot occurs faster at lower osmotic pressures. Scale bar, 2μm. (e) CD signal at 222 nm showing a constant decrease for PEG and ficoll but not glycerol at increasing wt% (left and upper right). Corresponding partitioning coefficient for glycerol, PEG, and ficoll (lower right).

Fig. 4. Nuclear and cytoplasmic YAP droplets selectively enrich and exclude different proteins. (a, b) Live-cell imaging showing colocalization of cytoplasmic EGFP-YAP droplets with mCherry-Dcp1a droplets (a), mCherry-NLK droplets (b) after hyperosmotic shock. (c) Live-cell imaging showing colocalization of cytoplasmic mCherry-YAP droplets with EGFP-LATS1 droplets after hyperosmotic shock. (d, e) Quantification of (a-b) and (c), respectively. Unpaired t test comparing PEG or Washed colocalizations with pre-treatment. Error bars show SEM. (f-h) Immunofluorescence images of nuclear EGFP-YAP with endogenous TEAD1 (f), β-catenin (g), and RNA Pol II (h) in control medium or in PEG medium. (i) Immunofluorescence image of EGFP-YAP with RNA-

FISH against Ctgf RNA, in control or in PEG medium. (j) Quantification of (f-h). Unpaired t tests comparing PEG with control-treated cells. (k) Quantification of EdU incorporation within 2hrs, after treating cells first with control medium for 10min or 10%PEG for 10min.

Fig. 5. Phase separation of YAP is important for its nuclear localization and signaling. (a) Disorder analysis of YAP 454aa isoform. Algorithms used: IUPred (blue), VLXT (cyan) and VSL2 (magenta). (b) Schematic of wild-type (WT) and mutant YAP structures. (c) Phase separation of EGFP-YAP variants in cell. (d) Percentage of cells expressing EGFP-YAP variants with liquid droplets at different time after PEG treatment. (e) Nuclear localization of different EGFP-YAP variants. (f) Relative localization of EGFP-YAP-ΔTAD with TEAD1 before and after PEG treatment. Immunofluorescence (g) Relative Ctgf mRNA expression in EGFP-YAP and EGFP-YAP-ΔTAD mutant after control or PEG treatment. Error bars show SEM.

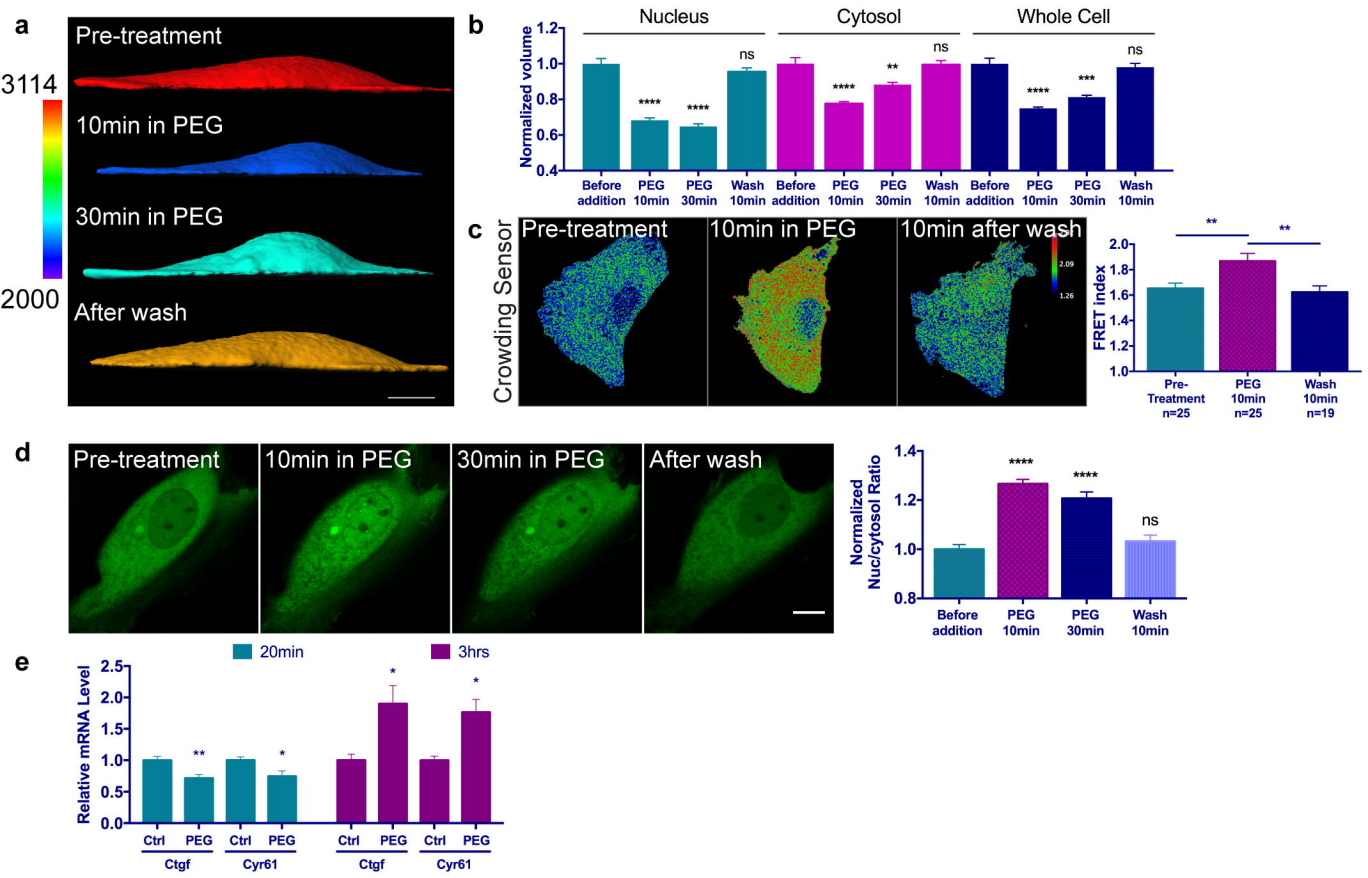
a
Pre-treatment
3114
10min in PEG
30min in PEG
2000
After wash
b
Nucleus
Cytosol
Whole Cell
Normalized volume
1.2
1.0
0.8
0.6
0.4
ns
****
****
**
***
Before addition
PEG 10min
PEG 30min
Wash 10min
c
Crowding Sensor
Pre-treatment
10min in PEG
10min after wash
2.09
1.26
FRET index
2.0
1.8
1.6
1.4
1.2
1.0
**
**
Pre-Treatment n=25
PEG 10min n=25
Wash 10min n=19
d
Pre-treatment
10min in PEG
30min in PEG
After wash
Normalized Nuc/cytosol Ratio
1.4
1.2
1.0
0.8
****
****
ns
Before addition
PEG 10min
PEG 30min
Wash 10min
e
20min
3hrs
Relative mRNA Level
2.5
2.0
1.5
1.0
0.5
0.0
**
*
*
*
Ctrl
PEG
Ctgf
Cyr61

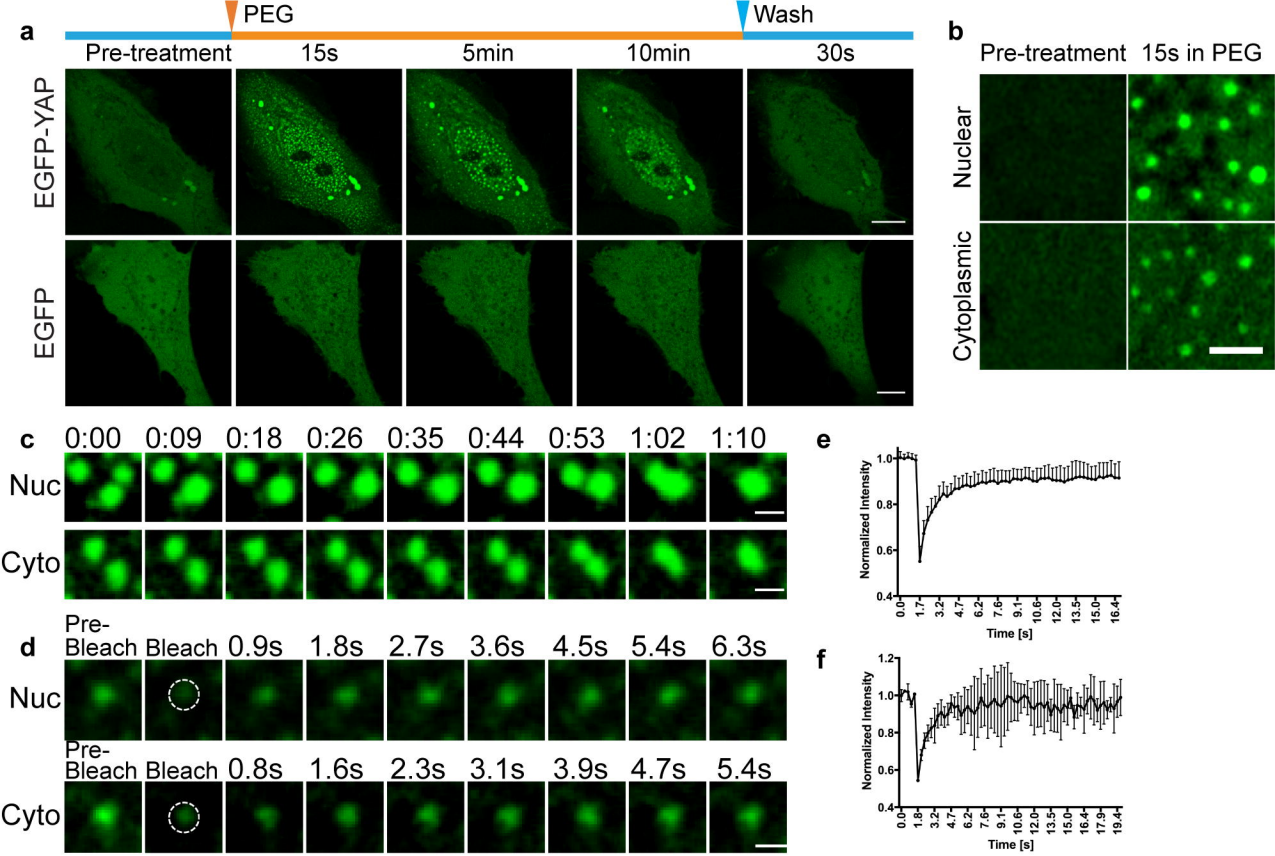
a
PEG
Wash
Pre-treatment
15s
5min
10min
30s
EGFP-YAP
EGFP
b
Pre-treatment
15s in PEG
Nuclear
Cytoplasmic
c
0:00
0:09
0:18
0:26
0:35
0:44
0:53
1:02
1:10
Nuc
Cyto
d
Pre-Bleach
Bleach
0.9s
1.8s
2.7s
3.6s
4.5s
5.4s
6.3s
Nuc
Pre-Bleach
Bleach
0.8s
1.6s
2.3s
3.1s
3.9s
4.7s
5.4s
Cyto
e
Normalized Intensity
Time [s]
f
Normalized Intensity
Time [s]

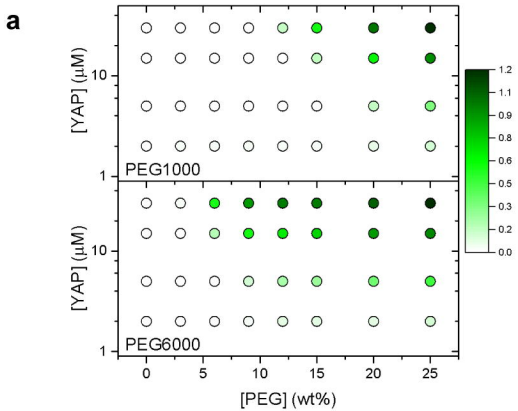
a
[YAP] (μM)
PEG1000
PEG6000
[PEG] (wt%)

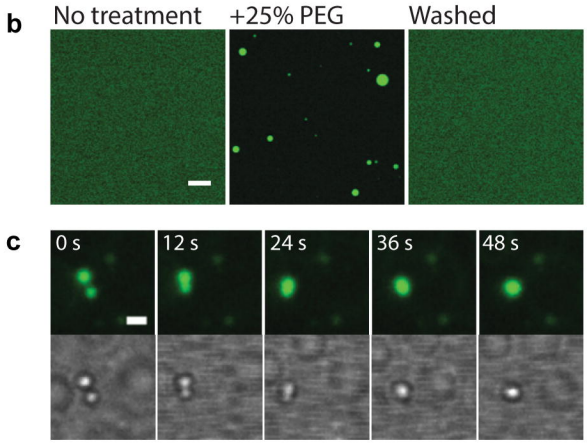
b
No treatment
+25% PEG
Washed
c
0 s
12 s
24 s
36 s
48 s

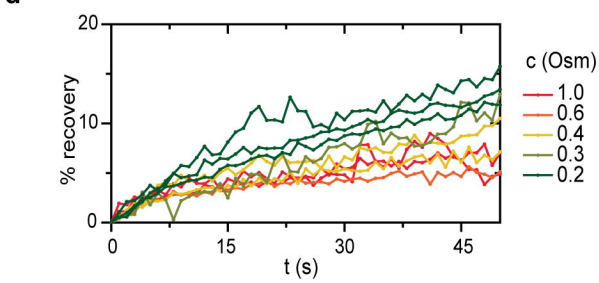
d
% recovery
t (s)
c (Osm)
1.0
0.6
0.4
0.3
0.2

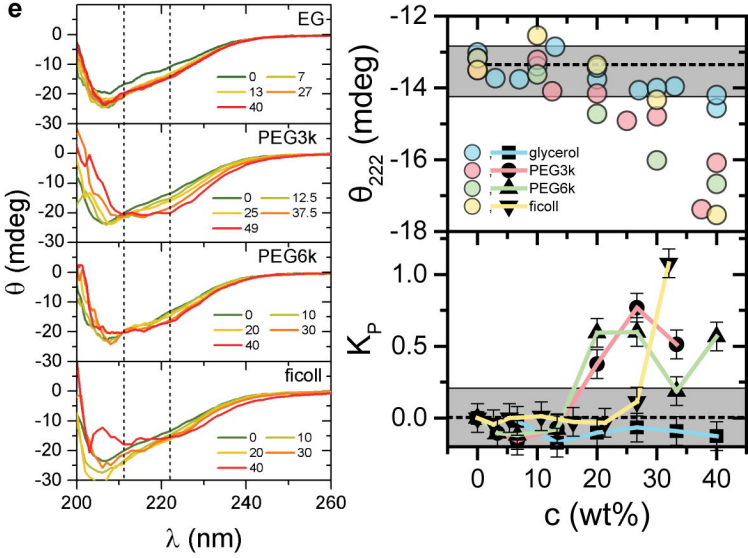
e
EG
PEG3k
PEG6k
ficoll
θ (mdeg)
λ (nm)
θ222 (mdeg)
glycerol
PEG3k
PEG6k
ficoll
KP
c (wt%)

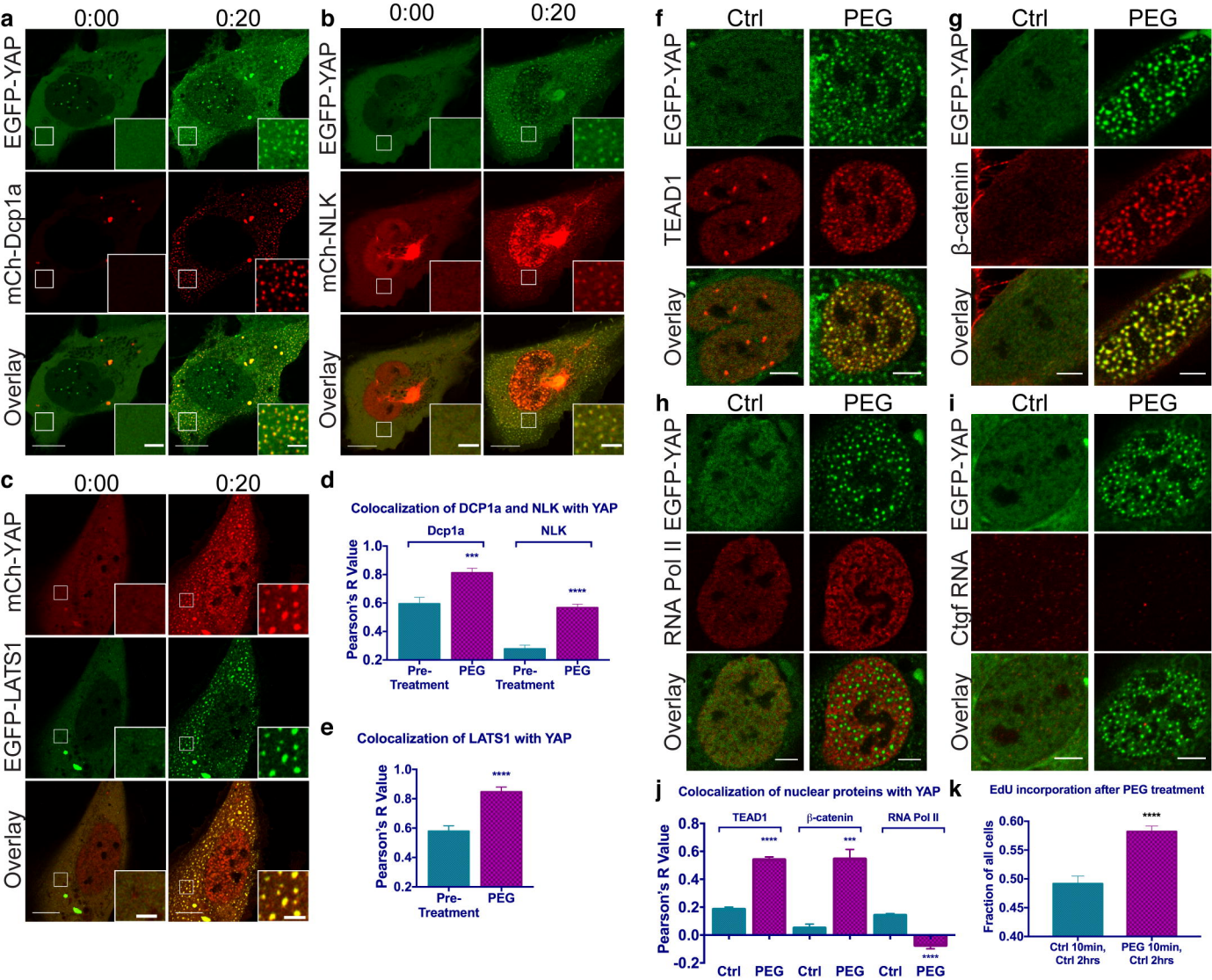
a
0:00
0:20
EGFP-YAP
mCh-Dcp1a
Overlay
b
0:00
0:20
EGFP-YAP
mCh-NLK
Overlay
c
0:00
0:20
mCh-YAP
EGFP-LATS1
Overlay
d
Colocalization of DCP1a and NLK with YAP
Dcp1a
NLK
Pearson's R Value
1.0
0.8
0.6
0.4
0.2
***
****
Pre-Treatment
PEG
Pre-Treatment
PEG
e
Colocalization of LATS1 with YAP
Pearson's R Value
1.0
0.8
0.6
0.4
0.2
****
Pre-Treatment
PEG
f
Ctrl
PEG
EGFP-YAP
TEAD1
Overlay
g
Ctrl
PEG
EGFP-YAP
β-catenin
Overlay
h
Ctrl
PEG
EGFP-YAP
RNA Pol II
Overlay
i
Ctrl
PEG
EGFP-YAP
Ctgf RNA
Overlay
j
Colocalization of nuclear proteins with YAP
TEAD1
β-catenin
RNA Pol II
Pearson's R Value
0.8
0.6
0.4
0.2
0.0
-0.2
****
***
****
Ctrl
PEG
Ctrl
PEG
Ctrl
PEG
k
EdU incorporation after PEG treatment
Fraction of all cells
0.60
0.55
0.50
0.45
0.40
****
Ctrl 10min, Ctrl 2hrs
PEG 10min, Ctrl 2hrs

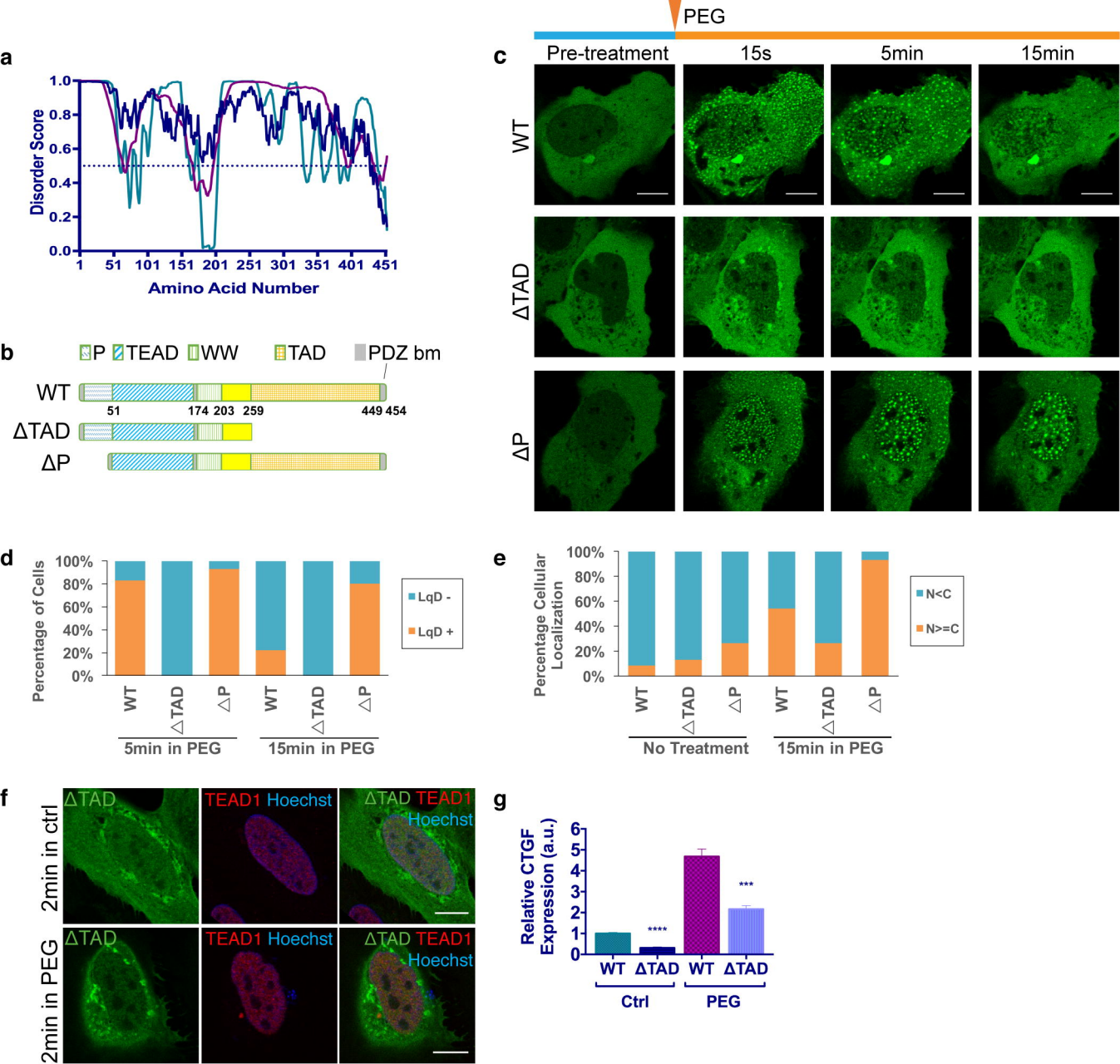
a
Disorder Score
1.0
0.8
0.6
0.4
0.2
0.0
1
51
101
151
201
251
301
351
401
451
Amino Acid Number
b
P
TEAD
WW
TAD
PDZ bm
WT
51
174
203
259
449
454
ΔTAD
ΔP
c
PEG
Pre-treatment
15s
5min
15min
WT
ΔTAD
ΔP
d
Percentage of Cells
100%
80%
60%
40%
20%
0%
LqD -
LqD +
WT
△TAD
△P
WT
△TAD
△P
5min in PEG
15min in PEG
e
Percentage Cellular Localization
100%
80%
60%
40%
20%
0%
N<C
N>=C
WT
△TAD
△P
WT
△TAD
△P
No Treatment
15min in PEG
f
ΔTAD
TEAD1 Hoechst
ΔTAD TEAD1 Hoechst
2min in ctrl
2min in PEG
g
Relative CTGF Expression (a.u.)
6
5
4
3
2
1
0
****
***
WT
ΔTAD
WT
ΔTAD
Ctrl
PEG